

Dynamics of Biological Macromolecules: Not a Simple Slaving by Hydration Water

S. Khodadadi,[†] J. H. Roh,^{‡§¶} A. Kisliuk,^{||} E. Mamontov,^{††} M. Tyagi,^{‡¶} S. A. Woodson,[§] R. M. Briber,[‡] and A. P. Sokolov^{||†‡*}

[†]Department of Polymer Science, University of Akron, Akron, Ohio; [‡]Department of Materials Science and Engineering, University of Maryland, College Park, Maryland; [§]T. C. Jenkins Department of Biophysics, The Johns Hopkins University, Baltimore, Maryland; [¶]Center for Neutron Research, National Institute of Standards and Technology, Gaithersburg, Maryland; ^{||}Chemical Sciences Division and ^{††}Spallation Neutron Source, Oak Ridge National Laboratory, Oak Ridge, Tennessee; and ^{‡‡}Department of Chemistry, University of Tennessee, Knoxville, Tennessee

ABSTRACT We studied the dynamics of hydrated tRNA using neutron and dielectric spectroscopy techniques. A comparison of our results with earlier data reveals that the dynamics of hydrated tRNA is slower and varies more strongly with temperature than the dynamics of hydrated proteins. At the same time, tRNA appears to have faster dynamics than DNA. We demonstrate that a similar difference appears in the dynamics of hydration water for these biomolecules. The results and analysis contradict the traditional view of slaved dynamics, which assumes that the dynamics of biological macromolecules just follows the dynamics of hydration water. Our results demonstrate that the dynamics of biological macromolecules and their hydration water depends strongly on the chemical and three-dimensional structures of the biomolecules. We conclude that the whole concept of slaving dynamics should be reconsidered, and that the mutual influence of biomolecules and their hydration water must be taken into account.

INTRODUCTION

It is well recognized that the dynamics of biological macromolecules, such as proteins, DNA, and RNA, plays a key role in their function. Yet, understanding the microscopic mechanisms of biomolecular motion remains a great challenge. Experimental and computational studies have demonstrated that hydration water and other solvents play a significant role in protein dynamics and activity (1–5). For example, dehydrated biomolecules have strongly suppressed dynamics and usually exhibit no biological activity (1–4). Once the hydration shell is completed, protein activity is restored and almost reaches the level of activity in solution (2).

In their pioneering works, Beece et al. (1) and Frauenfelder et al. (3) proposed that the solvent “slaves” the biological molecule, in the sense that the biomolecule dynamics and activity follow the solvent dynamics. Indeed, the results of many experimental studies supported this simple picture and demonstrated a strong coupling between protein and solvent dynamics (3,6–9). These results led to the idea that the solvent dynamics controls (i.e., slaves) the dynamics of the biological macromolecule. The mechanism of this dynamical coupling remains the subject of active discussion. It has been ascribed to protein-solvent hydrogen-bonding lifetimes (10,11) and/or to solvent translational motion (10,12,13). In particular, simulations using a dual heat-bath method in which the temperature of the solvent and the protein were controlled independently demonstrated that

protein dynamics is strongly affected by the hydration water temperature (13). In all of these studies (10–13), it was emphasized that the dynamics of the hydration water controls the dynamics of the biological macromolecules. In other studies, similar solvent-controlled protein dynamics was observed in viscous solvents, including glycerol and trehalose (9,11,14). However, these studies did not analyze the influence of the biological molecules on the dynamics of the surrounding solvent. Is the solvent really the “master” and the biomolecules just “slaves”, or are the behaviors coupled? We sought to address this question by experimentally studying the dynamics of different biomolecules in similar environments.

In this work, we analyzed hydrated tRNA dynamics using neutron scattering and dielectric relaxation spectroscopy. A comparison of the tRNA data with results obtained in earlier studies of hydrated protein and DNA reveals a strong difference in the dynamics and temperature variation for each biomolecule. Moreover, our analysis reveals that the hydration water dynamics also depends strongly on the biomolecule. These results call for a revision of the traditional picture of solvent-slaved dynamics and emphasize that the chemical and three-dimensional structures of the biomolecules affect not only their behavior but also that of the hydration water.

MATERIALS AND METHODS

Wheat-germ tRNA from Sigma-Aldrich (R7876) was purified with phenol and chloroform, and then dialyzed and lyophilized. After lyophilization, all exchangeable H-atoms in tRNA were replaced with D-atoms in 10 mM deuterated Na-cacodylate and 10 mM MgCl₂, and the sample was lyophilized again. The lyophilized deuterium-exchanged tRNA was hydrated under

Submitted October 15, 2009, and accepted for publication December 4, 2009.

*Correspondence: sokolov@utk.edu

Editor: Josh Wand.

© 2010 by the Biophysical Society
0006-3495/10/04/1321/6 \$2.00

doi: 10.1016/j.bpj.2009.12.4284

isopiestic conditions at 100% relative humidity in a desiccator with 99.9% D₂O. Different incubation times provided varying hydration levels ($h = 0.35$, 0.50, and 0.65 g water per gram of tRNA, determined by thermogravimetric analysis). For a more detailed description of the sample preparation, see Roh et al. (15). Similar samples (deuterium-exchanged tRNA hydrated with D₂O to the level $h \sim 0.6$ –0.65) were used for the dielectric measurements.

Neutron scattering measurements were performed using the high-flux back-scattering spectrometer (HFBS) at the NIST Center for Neutron Research in the energy range of $\pm 17 \mu\text{eV}$ ($\pm 4 \text{ GHz}$) with a resolution of $\sim 0.8 \mu\text{eV}$ ($\sim 0.24 \text{ GHz}$), and the backscattering silicon spectrometer (BASIS) at the Oak Ridge National Laboratory Spallation Neutron Source in the energy range of $\pm 250 \mu\text{eV}$ ($\pm 60 \text{ GHz}$) with a resolution of $\sim 10 \mu\text{eV}$ ($\sim 2.4 \text{ GHz}$). Three samples with different hydration levels were measured on the HFBS at $T = 300 \text{ K}$, 250 K, 225 K, 200 K and 10 K. Only the sample with $h = 0.65$ was measured on the BASIS at $T = 300 \text{ K}$, 275 K, 250 K, 225 K, 200 K, and 10 K. The combination of these two spectrometers allowed us to cover spectra over a broad frequency range (from $\sim 0.24 \text{ GHz}$ up to $\sim 60 \text{ GHz}$). The accessible range of the scattering wave vector, Q , for both spectrometers was $\sim 0.25 \text{ \AA}^{-1} < Q < 1.75 \text{ \AA}^{-1}$. The spectra were corrected for background and detector efficiency. Because the sample transmission was higher than $\sim 90\%$, no multiple-scattering corrections were applied.

Dielectric spectra in the frequency range between 10^{-2} Hz and 10^7 Hz were measured using the Concept 80 system from Novocontrol (Alpha-analyzer). Samples were placed between two gold-coated, parallel-plate electrodes with a Teflon spacer. To minimize the evaporation of water, an external Teflon ring was used to seal the samples. A capacitor with the sample was placed in a cryostat. The temperature was stabilized using a nitrogen gas flow and a Novocontrol Quatro temperature controller. Measurements were done every 5 K in the temperature range of 153–253 K. Measurements were repeated at a few temperatures to verify reproducibility, and no significant differences were observed. The samples were weighed before and after the measurements, and no significant water loss was observed.

RESULTS

Analysis of the neutron scattering spectra measured at different Q -values did not reveal any significant Q -dependence in the width of the quasielastic scattering, consistent with our earlier data (15). To improve the statistics, we summed the spectra measured at different Q -values. Fig. 1 presents the summed spectra for tRNA at different levels of hydration measured with HFBS at two different temperatures. The quasielastic intensity decreased strongly at lower temperatures and hydration levels. Fig. 2 shows the spectra of tRNA with $h = 0.65$ measured using the BASIS. The data show that the quasielastic scattering of tRNA is barely measurable at $T = 225 \text{ K}$. This is in strong contrast to the neutron scattering spectra of proteins, which exhibit significant quasielastic scattering even at $T = 200 \text{ K}$ (16). This difference between proteins and tRNA was previously emphasized (17) and ascribed to the strong contribution of methyl-group dynamics to the neutron scattering spectra of proteins (16–18). In contrast to proteins, where methyl H-atoms contribute $\sim 25\%$ of the incoherent neutron scattering, tRNA has only very small numbers of methyl groups, which contribute to $\sim 3\%$ of the scattering (15).

Analyzing the scattering data presented as susceptibility (instead of the dynamic structure factor) provides many advantages (for details, see Roh et al. (16)), such as the possi-

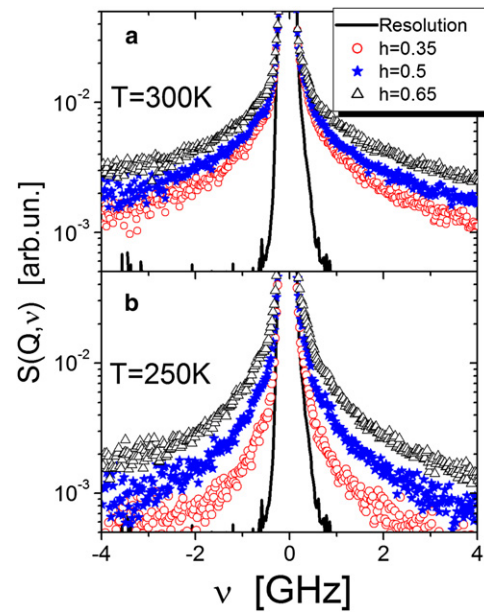


FIGURE 1 Quasielastic neutron scattering spectra of tRNA hydrated with D₂O to different levels of hydration h measured with HFBS at $T = 300 \text{ K}$ (a) and $T = 250 \text{ K}$ (b). The spectrum measured at $T = 10 \text{ K}$ presents the resolution function of HFBS. The spectra present a sum over all Q -values. Some of the data are from an earlier publication (15).

bility of directly comparing the scattering data with the dielectric loss spectra $\epsilon''(\nu)$. The neutron scattering data are presented as susceptibility spectra in Fig. 3, $\chi''(Q, \nu) \propto S(Q, \nu)/n_B(\nu) \approx S(Q, \nu)h\nu/kT$. Here $n_B(\nu) = [\exp(h\nu/kT) - 1]^{-1}$ is the Bose temperature factor, which in the classical limit (in our case, $h\nu \ll kT$) is simply $h\nu/kT$. The combined HFBS and BASIS neutron scattering susceptibility spectrum of completely hydrated tRNA ($h = 0.65$) at $T = 300 \text{ K}$ shows a broad symmetrically stretched peak with a maximum at a frequency of $\nu_{\text{max}} \sim 5$ –6 GHz (Fig. 3). The peak frequency provides a direct estimate of the characteristic relaxation time $\tau = (2\pi\nu_{\text{max}})^{-1}$. The peak shifts to lower frequency

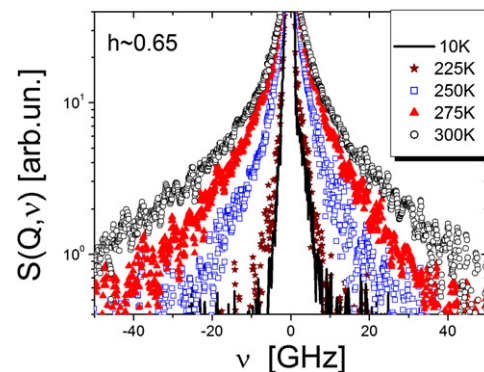


FIGURE 2 Quasielastic neutron scattering spectra of tRNA hydrated with D₂O to $h \sim 0.65$, measured at different temperatures with BASIS. The spectrum measured at $T = 10 \text{ K}$ presents the resolution function. The spectra present a sum over all Q -values.

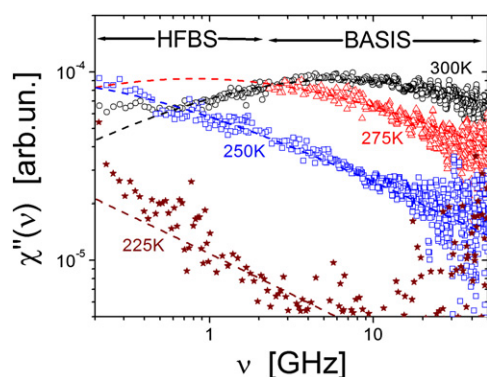


FIGURE 3 Neutron scattering susceptibility spectra of tRNA hydrated to $h \sim 0.65$ at different temperatures (shown by numbers). The spectra are combined by matching HFBS spectra at lower frequencies to the BASIS data. Symbols are experimental data, and dashed lines are fits to Eq. 1.

with decreasing temperature, reflecting the slowing down of the tRNA dynamics with cooling. The peak disappears from the accessible energy window at $T = 250$ K. This is in contrast to the lysozyme dynamics, where the peak in $\chi''(\nu)$ remains well resolved at $T = 250$ K (19). This clearly indicates that the dynamics of hydrated tRNA at $T = 250$ K is significantly slower than the dynamics of hydrated lysozyme.

For a quantitative analysis, we fit the susceptibility spectrum at $T = 300$ K using the Cole-Cole distribution function:

$$\chi''(\omega) = \chi_0 \frac{(\omega\tau)^{1-\alpha} \cos \frac{\alpha\pi}{2}}{1 + 2(\omega\tau)^{1-\alpha} \sin \frac{\alpha\pi}{2} + (\omega\tau)^{2-2\alpha}} \quad (1)$$

Here $\omega = 2\pi\nu$ is the angular frequency and α is the stretching parameter. The fit gives $\alpha = 0.5 \pm 0.05$ and $\tau = 26 \pm 6$ ps for the spectrum at $T = 300$ K. The maximum in the susceptibility spectra is not observed at other temperatures for which we have data. To fit the data, we assume that the amplitude of the relaxation spectrum χ_0 does not change with temperature (which is typical behavior for a relaxation process). The relaxation time at each temperature was estimated by fitting the spectra to Eq. 1 (Fig. 3). The fit at $T = 250$ K gives the stretching exponent as $\alpha \sim 0.45 \pm 0.05$, which is slightly lower than at $T = 300$ K. Fixing the exponent to $\alpha = 0.5$, however, does not significantly affect the estimated τ .

The estimated characteristic relaxation times of tRNA as a function of temperature are presented in Fig. 4. Throughout this work, error bars represent the standard deviation. Large error bars at temperatures of 250 K and 225 K are caused by the scattering in the data in the spectra and the shift of the relaxation peak out of the accessible energy window. Fig. 4 also presents relaxation times estimated previously from neutron scattering studies of hydrated lysozyme (19) and hydrated DNA (20). The comparison clearly demonstrates that hydrated protein has the fastest dynamics with the weakest temperature variation, and hydrated DNA has

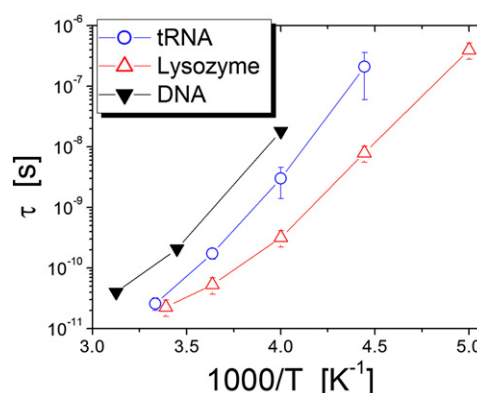


FIGURE 4 Temperature dependence of characteristic relaxation times estimated from the neutron scattering spectra of hydrated tRNA ($h \sim 0.65$), lysozyme ($h \sim 0.4$ (21)), and DNA ($h \sim 0.65$ (20)).

the slowest dynamics. The relaxation times of hydrated tRNA are between those of hydrated lysozyme and hydrated DNA.

The dielectric relaxation spectra of hydrated tRNA (Fig. 5) exhibit two clear processes: one with a strong amplitude at lower frequencies and one with a smaller amplitude at higher frequencies. Using WinFIT software provided by Novocontrol, we fit the spectra with two Havriliak-Negami distribution functions and a tail describing conductivity, contact polarization, and a possible slower relaxation process:

$$\epsilon^* = \epsilon_\infty + \sum_j \frac{\Delta\epsilon_j}{(1 + (i\omega\tau_j)^\alpha)^\beta} - i \frac{A}{\omega^s}, j = 1, 2 \quad (2)$$

Here A is the tail amplitude, s is the exponent describing the tail slope (which is different for the real and imaginary parts), τ is the characteristic relaxation time, $\Delta\epsilon$ is the dielectric strength, and α and β are the stretching parameters.

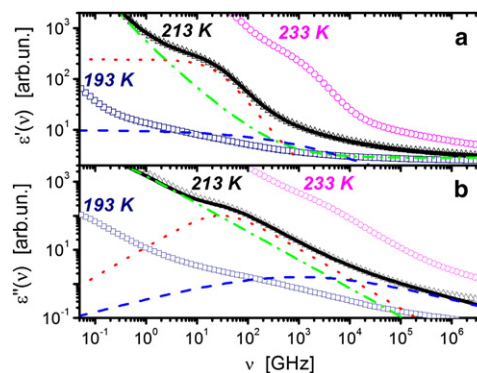


FIGURE 5 Dielectric spectra of hydrated tRNA at different temperatures: (a) real part $\epsilon'(\nu)$ and (b) imaginary part $\epsilon''(\nu)$. Symbols are experimental data, and lines show fits of the spectra at $T = 213$ K to Eq. 2. Solid line: fit of the total spectrum; dashed line: faster process; dotted line: slower process; dashed-dotted line: tail that includes slower processes, conductivity, contact polarization, and ϵ_∞ .

Details of the fit procedure can be found in our previous publication on dielectric studies of hydrated lysozyme (21). The fits yield the stretching parameters for the faster process as $\alpha = 0.46 \pm 0.1$, $\beta = 0.99 \pm 0.1$, and the stretching parameters for the slower process as $\alpha = 0.94 \pm 0.06$, $\beta = 0.99 \pm 0.01$. The spectral shapes of both processes appear to be symmetric (i.e., they are well approximated by the Cole-Cole distribution function). The fast process is strongly stretched, whereas the slower process has an almost Debye-like shape ($\alpha \sim 1$). The characteristic relaxation times were estimated from the maximum in the fits of the loss spectra $\tau = (2\pi\nu_{\max})^{-1}$.

Fig. 6 presents the estimated dielectric relaxation times of the hydrated tRNA. The faster process is relatively broad and has low amplitude (Fig. 5). As a result, the fit of the spectra for this process provides estimates of τ with large error bars. We repeated the dielectric measurements on three tRNA samples hydrated to the same hydration level ($h \sim 0.6$ – 0.65). Fig. 6 presents the data averaged over those three measurements, as well as the dielectric relaxation data for hydrated lysozyme and myoglobin (21,22). Consistent with the neutron scattering data (Fig. 4), the dielectric relaxation is faster and less temperature-dependent in hydrated proteins than in hydrated tRNA (Fig. 6).

DISCUSSION

The characteristic relaxation time in hydrated tRNA shows non-Arrhenius temperature dependence (Fig. 6), a well-known behavior for relaxation in various glass-forming systems and polymers. We start the discussion from the analysis of the neutron scattering data (Fig. 4). Due to the extremely high incoherent neutron scattering cross-section of the hydrogen atoms, the neutron scattering spectra of biological macromolecules hydrated with D_2O reflect the motions of the macromolecules. The incoherent neutron scattering cross-section of nonexchangeable H-atoms of

tRNA hydrated at 0.65 h contributes $\sim 70\%$ of the total (coherent and incoherent) neutron scattering cross-section from all nuclei, including D_2O . The total coherent and incoherent neutron scattering from D_2O in this sample contributes only $\sim 20\%$ of the total neutron scattering. Therefore, the observed relaxation process can be clearly assigned to motions of tRNA.

The experimental data suggest that relaxation in hydrated tRNA around ambient temperature occurs only slightly more slowly than in hydrated lysozyme (Fig. 4). As the temperature is lowered, however, the tRNA dynamics slow down more than the lysozyme dynamics, such that the difference in their relaxation times is >10 -fold at $T = 225$ K (Fig. 4). On the other hand, although the relaxation time is slower in DNA than in tRNA at room temperature, it seems to exhibit similar temperature variations.

The interpretation of dielectric relaxation spectra is not straightforward and remains a subject of discussion (21–25). The faster process is traditionally ascribed to the dynamics of hydration water (22–25), whereas the slower process is ascribed either to tightly bound hydration water (23) or to the motion of biological macromolecules (21,22,25). Since a discussion of the slow dielectric process is beyond the scope of this article, we will focus on an analysis and interpretation of the faster process.

The relaxation times of the fast dielectric relaxation process in tRNA agree with τ estimated from the neutron scattering spectra in the narrow temperature range where the data overlap (Fig. 6). Also, the stretching parameters of the relaxation processes observed in dielectric spectra and in neutron scattering spectra are similar. These similarities suggest that both techniques measure the same relaxation process. On the basis of this result, we ascribe it to a coupled hydration water-tRNA relaxation process, in similarity to an earlier analysis of neutron and dielectric relaxation spectra of hydrated lysozyme (21) (Fig. 6).

The dielectric relaxation time and temperature dependence are similar in hydrated samples of lysozyme (21) and myoglobin (22) (Fig. 6). These are small globular proteins with a slight difference in secondary structure (five α -helices and three β -sheets in lysozyme, and eight α -helices in myoglobin). However, the relaxation behavior of hydrated tRNA differs significantly from that observed in proteins (Fig. 6). This difference cannot be ascribed to the difference in hydration level. Both biomolecules are hydrated to the level that corresponds to complete hydration ($h \sim 0.65$ for tRNA and $h \sim 0.4$ for lysozyme). The difference in h corresponds to the different solvent-accessible surface area of these biomolecules (for details, see Roh et al. (15)). Dehydration of tRNA leads to narrowing of the quasielastic scattering spectrum (Fig. 1) (15). Thus, the relaxation time of tRNA at $h \sim 0.4$ is even slower than at $h \sim 0.65$. Thus, the difference in the observed relaxation times and temperature dependence (Figs. 4 and 6) is caused by chemical and structural differences among the proteins, tRNA, and DNA. This

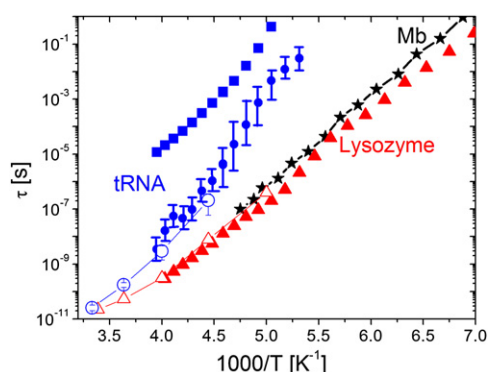


FIGURE 6 Temperature dependence of the characteristic relaxation time in hydrated tRNA: (■) slow dielectric relaxation process, (●) fast dielectric relaxation process, and (○) neutron scattering. For comparison, dielectric relaxation (▲) and neutron scattering (△) data for lysozyme (21) and dielectric relaxation data (stars) for myoglobin (22) are presented.

conclusion contradicts the traditional view that the dynamics of biological macromolecules is slaved by the dynamics of the solvent. According to the concept of slaved dynamics, all three biomolecules should have had similar temperature dependence as dictated by the dynamics of the hydration water. This is clearly not the case.

Instead, we propose that the specific biomolecular structure plays an important role in the overall dynamics, even when different biomolecules exposed to the same solvent (water) are compared. The observed dynamics of the system come from the mutual coupling of the motions in the biomolecule and the solvent. An important test of this idea is to determine whether the dynamics of hydration water is also affected by the biomolecules. The most efficient way to study the dynamics of hydration water is to use completely deuterated proteins. Such studies have been initiated and the results demonstrated a similarity between the dynamics of hydration water and that of proteins (26–28). Unfortunately, no such studies have been done for lysozyme, tRNA, or DNA. However, Chen and co-workers have extensively studied the dynamics of hydration water surrounding different biomolecules (29–31). To separate the contribution of hydration water, they acquired neutron scattering spectra of biomolecules hydrated in H₂O and in D₂O. Their measurements were performed at lower hydration levels ($h \sim 0.3$ for lysozyme and $h \sim 0.5$ for RNA and DNA (29–31)), which precludes a direct comparison of their results with our data. Nonetheless, the results of Chen and co-workers show that lysozyme hydration water has the fastest dynamics, DNA has the slowest, and tRNA is in between (Fig. 7). This conclusion agrees well with our results (Fig. 5), implying that the relaxation behavior of the hydration water is affected by the biomolecules.

The observed difference in the relaxation behavior can be explained by the difference in structure of the studied biomolecules. Lysozyme and myoglobin are globular proteins with a hydrophobic core that is isolated from the hydration water. Moreover, these proteins have a significant

number of methyl groups that plasticize the internal protein motions even in the dehydrated state (15,18,32,33). This might explain the faster dynamics of the hydrated proteins (Fig. 6) and weaker dependence of protein dynamics on hydration reported previously (15). On the other hand, tRNA and DNA lack a hydrophobic core. Water molecules enter the grooves of double helices and affect the dynamics of nucleic acids much more strongly than they affect that of globular proteins. DNA and tRNA also have small numbers of methyl groups. Therefore, the many internal methyl groups in proteins and less exposure of protein residues to the solvent lead to weaker temperature variation in the protein dynamics compared to the tRNA dynamics (Fig. 6). DNA has a rod-like structure that is more rigid than the structure of folded tRNA. This explains why the dynamics of DNA and its hydration water appears even slower than that of tRNA. It is also possible that ions associated with nucleic acids may have additional effects on hydration water dynamics. This question can be studied by analyzing water with different ions without biomolecules.

We want to add a brief comment related to the relaxation of hydration water at temperatures below $T \sim 225$ K. Neither the tRNA data presented here nor the earlier lysozyme and myoglobin data (Fig. 6) show the cusp-like behavior of τ around $T \sim 225$ K reported by Chen and co-workers for hydration water (29–31). Therefore, our results do not support the existence of the cusp-like, fragile-to-strong crossover proposed by them (29–31). This topic is beyond the scope of this work, but the interested reader can find more detailed discussions about it in earlier publications (19,34–36).

CONCLUSIONS

Analyses of neutron scattering and dielectric relaxation spectra identified a relaxation process that we ascribe to a coupled tRNA-hydration water relaxation. This process exhibits non-Arrhenius temperature dependence. A comparison of the results for hydrated tRNA with earlier data for hydrated lysozyme and DNA demonstrates significant differences in the dynamic behavior of these biomolecules. Moreover, the dynamics of hydration water also exhibits significant differences. Relaxation of globular proteins and their hydration water is faster and varies much more slowly with temperature compared to the dynamics of tRNA and its hydration water. The dynamics of DNA and its hydration water appears to be even slower than the tRNA dynamics. This indicates that the dynamics of the biomolecules is not simply slaved by the dynamics of the hydration water. The chemical and three-dimensional structures of the biomolecules play an important role. Moreover, the biomolecule affects the dynamics of the hydration water. Therefore, the concept of slaving dynamics should be reconsidered and a more complete model of coupled biomolecule-water dynamics should be developed.

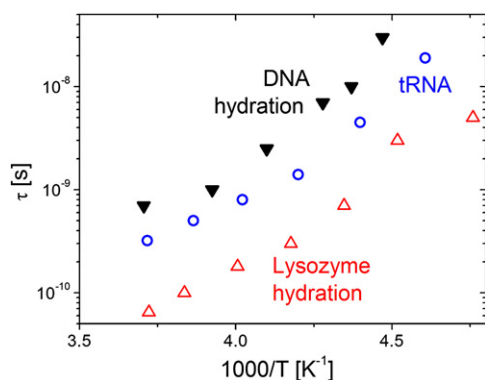


FIGURE 7 Characteristic relaxation times of hydration water estimated using neutron scattering spectroscopy. Data for hydration water of lysozyme at $h = 0.3$ (26), DNA at $h = 0.5$ (28), and tRNA at $h = 0.5$ (27) are shown.

The Akron team thanks the National Science Foundation for partial financial support (DMR-0804571). Part of the research conducted at the Oak Ridge National Laboratory's Spallation Neutron Source was sponsored by the Scientific User Facilities Division, Office of Basic Energy Sciences, US Department of Energy. This work utilized facilities supported in part by the National Science Foundation (DMR-0454672). The University of Maryland group acknowledges the support of the National Institute of Standards and Technology, US Department of Commerce.

REFERENCES

1. Beece, D., L. Eisenstein, ..., K. T. Yue. 1980. Solvent viscosity and protein dynamics. *Biochemistry*. 19:5147–5157.
2. Rupley, J. A., and G. Careri. 1991. Protein hydration and function. *Adv. Protein Chem.* 41:37–172.
3. Frauenfelder, H., P. W. Fenimore, and B. H. McMahon. 2002. Hydration, slaving and protein function. *Biophys. Chem.* 98:35–48.
4. Gabel, F., D. Bicout, ..., G. Zaccari. 2002. Protein dynamics studied by neutron scattering. *Q. Rev. Biophys.* 35:327–367.
5. Tsai, A. M., D. A. Neumann, and L. N. Bell. 2000. Molecular dynamics of solid-state lysozyme as affected by glycerol and water: a neutron scattering study. *Biophys. J.* 79:2728–2732.
6. Fenimore, P. W., H. Frauenfelder, ..., F. G. Parak. 2002. Slaving: solvent fluctuations dominate protein dynamics and functions. *Proc. Natl. Acad. Sci. USA*. 99:16047–16051.
7. Fenimore, P. W., H. Frauenfelder, ..., R. D. Young. 2004. Bulk-solvent and hydration-shell fluctuations, similar to α - and β -fluctuations in glasses, control protein motions and functions. *Proc. Natl. Acad. Sci. USA*. 101:14408–14413.
8. Diehl, M., W. Doster, ..., H. Schober. 1997. Water-coupled low-frequency modes of myoglobin and lysozyme observed by inelastic neutron scattering. *Biophys. J.* 73:2726–2732.
9. Caliskan, G., D. Mechtani, ..., I. Peral. 2004. Protein and solvent dynamics: how strongly are they coupled? *J. Chem. Phys.* 121:1978–1983.
10. Tarek, M., and D. J. Tobias. 2002. Role of protein-water hydrogen bond dynamics in protein dynamical transition. *Phys. Rev. Lett.* 88:138101.
11. Dirama, T. E., G. A. Carri, and A. P. Sokolov. 2005. Coupling between lysozyme and glycerol dynamics: microscopic insights from molecular dynamics simulations. *J. Chem. Phys.* 122:244910.
12. Vitkup, D., D. Ringe, ..., M. Karplus. 2000. Solvent mobility and the protein 'glass' transition. *Nat. Struct. Biol.* 7:34–38.
13. Tournier, A. L., J. Xu, and J. C. Smith. 2003. Translational hydration water dynamics drives the protein glass transition. *Biophys. J.* 85:1871–1875.
14. Paciaroni, A., S. Cinelli, and G. Onori. 2002. Effect of the environment on the protein dynamical transition: a neutron scattering study. *Biophys. J.* 83:1157–1164.
15. Roh, J. H., R. M. Briber, ..., A. P. Sokolov. 2009. Dynamics of tRNA at different levels of hydration. *Biophys. J.* 96:2755–2762.
16. Roh, J. H., J. E. Curtis, ..., A. P. Sokolov. 2006. Influence of hydration on the dynamics of lysozyme. *Biophys. J.* 91:2573–2588.
17. Caliskan, G., R. M. Briber, ..., A. P. Sokolov. 2006. Dynamic transition in tRNA is solvent induced. *J. Am. Chem. Soc.* 128:32–33.
18. Doster, W., and M. Settles. 2005. Protein-water displacement distributions. *Biochim. Biophys. Acta*. 1749:173–186.
19. Khodadadi, S., S. Pawlus, ..., A. P. Sokolov. 2008. The origin of the dynamic transition in protein. *J. Chem. Phys.* 128:195106.
20. Sokolov, A. P., J. H. Roh, ..., V. García Sakai. 2008. Role of hydration water in dynamics of biological macromolecules. *Chem. Phys.* 345:212–218.
21. Khodadadi, S., S. Pawlus, and A. P. Sokolov. 2008. Influence of hydration on protein dynamics: combining dielectric and neutron scattering spectroscopy data. *J. Phys. Chem. B*. 112:14273–14280.
22. Swenson, J., H. Jansson, and R. Bergman. 2006. Relaxation processes in supercooled confined water and implications for protein dynamics. *Phys. Rev. Lett.* 96:247802.
23. Miura, N., Y. Hayashi, and S. Mashimo. 1996. Hinge-bending deformation of enzyme observed by microwave dielectric measurement. *Biopolymers*. 39:183–187.
24. Nandi, N., K. Bhattacharyya, and B. Bagchi. 2000. Dielectric relaxation and solvation dynamics of water in complex chemical and biological systems. *Chem. Rev.* 100:2013–2046.
25. Oleinikova, A., P. Sasisanker, and H. Weingartner. 2004. What can really be learned from dielectric spectroscopy of protein solutions? A case study of ribonuclease A. *J. Phys. Chem. B*. 108:8467–8474.
26. Gabel, F., and M. C. Bellissent-Funel. 2007. C-phycocyanin hydration water dynamics in the presence of trehalose: an incoherent elastic neutron scattering study at different energy resolutions. *Biophys. J.* 92:4054–4063.
27. Wood, K., A. Frölich, ..., M. Weik. 2008. Coincidence of dynamical transitions in a soluble protein and its hydration water: direct measurements by neutron scattering and MD simulations. *J. Am. Chem. Soc.* 130:4586–4587.
28. Paciaroni, A., A. Orecchini, ..., F. Sacchetti. 2008. Fingerprints of amorphous ice like behavior in the vibrational density of states of protein hydration water. *Phys. Rev. Lett.* 101:148104.
29. Chen, S. H., L. Liu, ..., E. Mamontov. 2006. Observation of fragile-to-strong dynamic crossover in protein hydration water. *Proc. Natl. Acad. Sci. USA*. 103:9012–9016.
30. Chu, X. Q., E. Fratini, ..., S. H. Chen. 2008. Observation of a dynamic crossover in RNA hydration water which triggers a dynamic transition in the biopolymer. *Phys. Rev. E*. 77:011908.
31. Chen, S. H., L. Liu, ..., E. Mamontov. 2006. Experimental evidence of fragile-to-strong dynamic crossover in DNA hydration water. *J. Chem. Phys.* 125:171103.
32. Roh, J. H., V. N. Novikov, ..., A. P. Sokolov. 2005. Onsets of anharmonicity in protein dynamics. *Phys. Rev. Lett.* 95:038101.
33. Krishnan, M., V. Kurkal-Siebert, and J. C. Smith. 2008. Methyl group dynamics and the onset of anharmonicity in myoglobin. *J. Phys. Chem. B*. 112:5522–5533.
34. Pawlus, S., S. Khodadadi, and A. P. Sokolov. 2008. Conductivity in hydrated proteins: no signs of the fragile-to-strong crossover. *Phys. Rev. Lett.* 100:108103.
35. Swenson, J., H. Jansson, J. Hedstrom, and R. Bergman. 2007. Properties of hydration water and its role in protein dynamics. *J. Phys.: Cond. Matter*. 19:205109.
36. Vogel, M. 2008. Origins of apparent fragile-to-strong transitions of protein hydration waters. *Phys. Rev. Lett.* 101:225701.